# Processing date kernels for iron (III) and chromium (VI) adsorption from water

Behzad Hossieni[1] , Somayeh Sohrabi*,[2,3] , Faranak Akhlaghian*,[1]

[1]Department of Chemical Engineering, Faculty of Engineering, University of Kurdistan, Sanandaj, Kurdistan, Iran.
[2]Chemical Engineering Faculty, Amirkabir University of Technology, Tehran Polytechnic, Tehran, Iran.
[3]Mechanical Engineering Faculty, Sharif University of Technology, Tehran, Iran.

## GRAPHICAL ABSTRACT
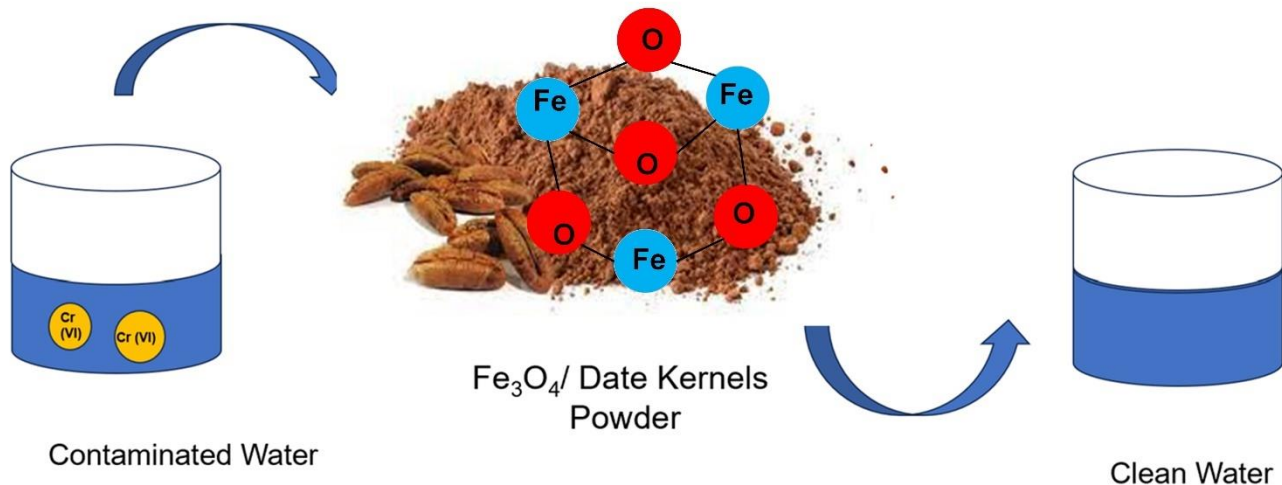


Contaminated Water — $Fe_3O_4$/ Date Kernels Powder — Clean Water

## ARTICLE INFO

## ABSTRACT

Inexpensive and new adsorbents, which are produced by processing the abundant agricultural by-products, can provide an efficient solution for a cleaner environment. The occurrence of heavy metals in water may pose a significant threat to human health. In this work, the processed date kernels are used to remove chromium (VI) and iron (III) from water. The XRD, FTIR, SEM, VSM and EDX techniques are used to characterize the adsorbents. The equilibrium adsorbent dose for iron is 2 g/L while for chromium (VI) it is 4 g/L and the equilibrium time is 20 min. Moreover, acidic conditions favored the adsorption for both targets. The adsorption experiments showed that the kinetics of adsorption of chromium (VI) and iron (III) on date kernel powder fitted the pseudo-second-order model. The optimum adsorption capacities for iron (III) and chromium (VI) are 10.5 mg/g and 0.66 mg/g, respectively. In the meantime, the remarkable efficiency of the date kernel-based adsorbent for iron (III) removal paves the way for designing new magnetic adsorbents.

## 1. Introduction

Nowadays, human industrial activities introduced heavy metals into the environment. This class of water contaminant is harmful owing to their ability to move in aquatic ecosystems as well as their toxicity. Since heavy metal ions cannot be decomposed or degraded, they are stable and permanent. The adverse impact of heavy metals is both acute and permanent (Lasat, 2002). The growth of iron bacteria deriving energy from ion oxidation can clog pipes, causing the water to be stagnate and disrupt the water supply system and treatment equipment (Qasim *et al.*, 2000). The World Health Organization (WHO) restricts the allowable

amount of iron in drinking water to <0.3 ppm (Ehralian *et al.*, 2016). Accumulation of chromium in animal and plant tissues poses serious risks, causing disorders in the liver, kidneys, and lungs. The World Cancer Society (WCS) has confirmed the carcinogenic potential of chromium (VI), setting the maximum allowable amount of chromium in drinking water is set at 0.01 ppm (Selvi and Kadirvelu, 2001).

Waste and wastewater from industries such as battery manufacturing, ceramics, electroplating, textile, tanning, dyeing, mining, refining operations, metal cladding, smelting and extraction of metals, and other small and large-scale metal processes can increase the local concentration of heavy metals in a geographical place

*Corresponding author Email: ssohrabi@aut.ac.ir;
fr.akhlaghian@uok.ac.ir

(Ahluwalia and Goyal, 2007). There are numerous methods for removing heavy metals from aqueous solutions, including reverse osmosis, filtration, chemical oxidation, reduction, activated carbon, membrane processes, ion exchange, coagulation, precipitation, electrolytic techniques, and electrochemical purification (Yunus Pamukoglu and Kargi, 2006). However, none of those mentioned above have succeeded in leading to the utilization of waste for removing pollutants with high efficiency. Among the available options, the adsorption technique has been extensively implemented for water treatment owing to its facile process, low energy use, simple maintenance, high adsorption capacity, high effectiveness and low price. Thus, scientists are actively seeking inexpensive adsorbents with easy recovery (Yang and Wang, 2006). For instance, Mohammed Saleh *et al.* (2021), synthesized zero -valent iron nanoparticles from Verbascum Thapsus leaves and used them for Cr (VI) adsorption. The complete removal of Cr (VI) has been attained at the pH value of 5.2 and a dose of 1 g/L after 30 min for an initial chrome concentration of 25 ppm. H. Shan et al. (2021) evaluated the efficiency of the iron oxide (Fe $O_x$) integrated with composites of graphene oxide/chitosan for Cr (VI) removal. Their findings showed that Fe (III) was a superior modifying material than Fe (II). Under the optimum circumstances, the chromium removal yield was 94.3%, and the maximum adsorption capacity was 83.8 mg/g. After five cycles with adsorbent regeneration, the chromium removal yield was 84%.

In another study, Jain et al. (2018), developed a composite of iron oxide and activated carbon and used it for water treatment. The optimum condition for Cr (VI) removal is strong acidic condition (pH = 2) and for Cu (II), and Cd (II) removal is weak acidic (pH = 6) condition. The equilibrium data of ion adsorption followed the Langmuir isotherm model.

Agricultural by-products and natural fibers such as skins and seeds of fruits, cereals, leaves and stems of plants, and sawdust from wood industries, as natural adsorbents are suitable options due to their availability, high adsorption capacity, and economic value (Pavan, Mazzocato, and Gushikem, 2008). Rice husk, with and without modifications, has been applied for chromium (VI) removal. Meanwhile, tea-based adsorbent eliminated nearly 70% of the hexavalent chromium into Cr (III) (Sabir *et al.*, 2021). Misbah Bashir et al. 2020 investigated copper adsorption onto low-cost natural adsorbents such as eggshells and tea leaves. They achieve more than 85 % efficiency with a high capacity of 420–450 mg/g (Bashir, Tyagi, and Annachhatre, 2020). In a study by Songlin Fan et al. 2020 sugarcane bagasse was used to prepare an adsorbent for the removal of $Pb^{2+}$ and $Cd^{2+}$ ions. Fan *et al.* prepared sugarcane succinate/$Ca^{2+}$/sugarcane succinate/alginate by layer-by-layer technology and used it to remove $Pb^{2+}$ and $Cd^{2+}$. The optimum adsorption capacities were 354.60 mg/ g and 176.36 mg/ g for $Pb^{2+}$ and $Cd^{2+}$, respectively (Fan, et al., 2020).

Further research work is expected on the application of promising agricultural-based adsorbents to treat real industrial effluents (Omo-Okoro, et al. 2018). According to the "Food and Agriculture Organization of the United Nations", more than 1.15 million tons of dates are produced in Iran. With its first rank, Iran stands out among the Asian date producers (Karizaki, 2017). Iran has a substantial capacity of date production, consequently, the date kernel is very abundant as waste, which can be used to remove heavy metals from water (Keramat and Khorvash, 2002).

This work introduces a green and facile method for recycling the date kernels into bio-sorbent, effectively managing agricultural waste and simultaneously removing water contaminants. Moreover, adsorption efficiency and kinetic models are assisted to evaluate iron and chrome removal. The effect of process variables, including pH, temperature, contact time, pollutant concentration, and adsorbent dosage has been investigated.

## 2. Materials and methods
### 2.1. Materials

To synthesize the adsorbents, (FeCl$_3$). 6 H$_2$O (98 %), FeSO$_4$ .7 H$_2$O (98 %), N$_2$H$_4$ (98 %), and Ammonia (25 %) were used, which were purchased from Merck company. Nitrogen gas is of industrial purity, the date is bought from the local market. Fe (NOO$_3$). 9 H$_2$O (50 %, Merck) and Potassium dichromate (K$_2$Cr$_2$O$_7$ , 50 %, Merck) were used to prepare stock solutions of iron and chrome, respectively. Moreover, Thioglycolic acid HSCH$_2$CO$_2$H, (Medicinal purity with European standard) and Ammonia (25 %, Merck) were used for visible spectroscopic detection of iron ions. Diphenyl carbazide ($C_{13}H_{14}N_4O$, 50%, Merck) and $H_2SO_4$ (95%, Merck) were used for visible spectroscopic detection of chrome ions.

### 2.2. Preparation of adsorbents

The considered pretreatment for date kernel powder (DKP) is physical. First, date kernels were rinsed with distilled water and soaked in it for 72 h. Afterward, they were dried in an oven at 100 ° C for 48 h. Finally, they were crushed and sieved with a mesh size of 170 to 90-106 μm particles.

The preparation methods of Fe$_3$O$_4$ and Fe$_3$O$_4$/ date kernel powder include physical and chemical steps. First, 100 ml of iron (III) chloride solution (0.875 M) and iron (II) sulfate (0.5 M) were mixed under a stoichiometric ratio of 1.75: 1 with the presence of nitrogen gas at 60 ° C. The only difference in Fe$_3$O$_4$ and Fe$_3$O$_4$/ date kernels powder synthesis is the addition of 4.5 g of date kernel powder in this step. After 10 min of mixing, two reagents (hydrazine hydrate (5 ml) and Ammonia (10 ml)) were gradually added drop by drop until a pH =9 was obtained. A black precipitate was obtained after mixing for 30 min. Afterward, the bio-adsorbent was rinsed several times with distilled water, and the pH reached 7. The final step is drying in an oven at 70 °C.

### 2.3. Batch adsorption experiments

The experiments on the removal of iron (III) and chromium (VI) from water were performed by adsorbents in a batch mode under constant-speed stirring using a magnetic stirrer to achieve equilibrium. Finally, the adsorbents were isolated from water by centrifugation and filtration and the iron and chrome concentration was measured using a spectrophotometer (T80+ model from PG Instruments Company). Removal efficiencies were calculated using the following Eq.1.

$$\text{Removal (\%)} = \frac{C_0 - C_f}{C_0} \times 100 \tag{1}$$

where C$_0$ and C$_f$ are the concentrations of the pollutant in solution at t=0 and t= t$_f$, respectively. The adsorption capacity (q$_e$) of the adsorbents at equilibrium time was calculated using Eq. 2.

$$q_e = \frac{(C_0 - C_e)V}{M} \tag{2}$$

where, $q_e$ is adsorption equilibrium capacity (mg/g), $C_0$ is initial concentration of adsorbent in solution (mg/L), $C_e$ is final concentration of adsorbent after equilibration (mg/L), V is Volume of liquid inside the reactor (L), M is adsorbent dose (g). To determine the concentration of iron and chrome in the aqueous solution, the Beer-Lambert law (Eq.3) is used:

$$log\,{}^{I_0}\!/_I = abc \tag{3}$$

where, "$I_0$" is the initial light intensity, "I" is the passing light intensity and the right side of the equation is the amount of matter absorbed, "a" is the absorption coefficient of the substance, "b" is the cell thickness in cm and "c" is the concentration in mol∕L. The Thioglycolic acid method was used to detect iron ions. First, 1 mL of thioglycolic acid was added to 50 ml of the standard solution and then placed in an oven at ℃ 100 for 30 min. The sample was then cooled to ambient temperature, and 2 ml of concentrated ammonia was added per 1 ml of thioglycolic acid, and after 2 min the corresponding absorbance was read at 530 nm (Swank and Mellon, 1938 and Lyons, 1927). Diphenyl carbazide was used to identify chromium. In this method, 10 ml of samples were mixed with 5 ml (0.5 N) sulfuric acid and then diluted with distilled water to a volume of 50 ml. To the resulting solution, 2 mL solutions of 1, 5 diphenyl carbazide were added, a very rapid reaction was formed, and a purple complex was formed. After 10 min, the absorbance of the samples was measured by a spectrophotometer (T80+ model from PG Instruments Company) at the wavelength of 540 nm (Andrew and Franson, 2005).

### 2.4. Characterization techniques

The FTIR test was used as a fingerprint of the adsorbents to identify the bonds and functional groups in the DKP sample. The so-called spectrum was recorded by a VECTOR22 (Bruker, Germany) FT-IR spectrophotometer. The surface morphology of the adsorbents was investigated by scanning electron microscope MIRA3 of the TESCAN Company at the acceleration voltage of 15.0 kV. The DKP, Fe$_3$O$_4$ and Fe$_3$O$_4$/DKP are characterized by X-ray diffraction (XRD) using DIFFRACTOMETER of inel CO. EQUINOX3000 model with Cu Ka radiation: 1.54190 A at 40 kV and 30 mA. The XRD patterns were collected from 10 to 80∘in 2ɵ at a scan rate of 0.032∘/s. For Fe$_3$O$_4$ and Fe$_3$O$_4$/DKP a vibrating sample magnetometer of kavir model is used.

## 3. Results and discussions
### 3.1. Characterization

In the XRD spectrums of date kernels powder, peaks at 16.1 ° and 20.2° are attributed to cellulose and hemicellulose hydrate. The peak at 25.4° is related to the crystalline structure of fatty acids in date kernels. The

peak at 33.3° is related to hemicellulose hydrate. Moreover, the XRD patterns of $Fe_3O_4$/Date Kernels adsorbent show $Fe_3O_4$ peaks, but the intensity of some peaks has been reduced with respect to pure $Fe_3O_4$. This result highlights the economic value of the adsorbent (Bhaumik *et al.*, 2011; Ghandoor *et al.*, 2012; Khan and Ahmad, 2022). The property of $Fe_3O_4$/Date Kernels and $Fe_3O_4$ are the same. It means that by less use of time and chemicals for $Fe_3O_4$ synthesis, we can have an adsorbent with similar property. So, a by- product of agriculture is not only not wasted, but it is used to remove environmental pollutants.
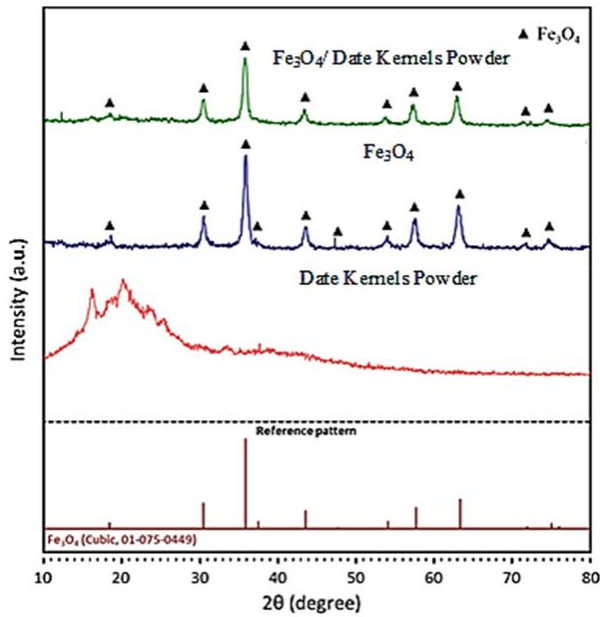


**Fig. 1.** XRD of DKP, $Fe_3O_4$ and $Fe_3O_4$/DKP.

To identify the functional groups of samples, the Fourier Transform Infrared (FT-IR) spectrum was recorded. Table 1 shows that the stretching O-H peaks around 3400 $cm^{-1}$ are associated with the water content in the samples during synthesis. At 2920 $cm^{-1}$, the peak is representative of methylene. At 1647.1 $cm^{-1}$ and 1633.6 $cm^{-1}$, an aromatic peak is detectable for DKP. Peaks in the 1350-1480 $cm^{-1}$ range can be associated with alkanes or saturated fatty acids in DKP. Some peaks in the range of 1050-1150 $cm^{-1}$ and 1210-1320 $cm^{-1}$ are fatty acids. The existence of fatty acids facilitates iron adsorption (Chernyshova *et al.* 2013). Peaks at 871.8 $cm^{-1}$, 810 $cm^{-1}$, and 812 $cm^{-1}$ are attributed to aromatic compounds (Salman and Abid, 2011).

**Table 1.** FTIR analysis of DKP.

| Functional group | Wave number, $cm^{-1}$ | Peaks of DKP, $cm^{-1}$ |
|---|---|---|
| $O-H$ | 3200-3400 | 3388.7 |
| $=CH_2$ | 2915-2935 | 2920 |
| $C=C$ | 1620-1680 | 1647.1 |
| $-C-H$ | 1350-1480 | 1448.4 |
| $C-O$ | 1050-1150 | 1066.23 |
| | 1210-1320 | 1249.78 |
| $=C-H$ | | 871.8 |
| $C-H$ | 675-900 | 810 |

Fig. 2 shows the adsorbents' morphology, highlighting the surface roughness of the surface of DKP in the SEM image. This finding shows that immobilization of nanoparticles on this surface is more than on smooth surfaces. Moreover, Fig. 2 represents the magnetic $Fe_3O_4$ nanoparticles, the inset corresponding diameter histogram. Fig. 2 shows that the $Fe_3O_4$ nanoparticles shape has been kept while its size is altered. In another word, during the immobilization process, the nanoparticles may aggregate so the histogram char indicates that the diameters are increased from $44.93\pm11.7$ nm to $103.18\pm 31.2$ nm.
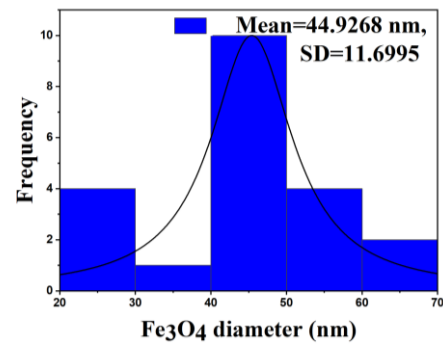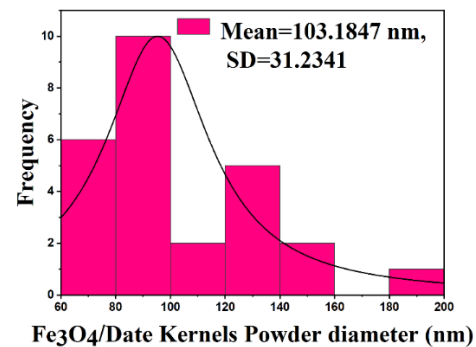


**(a)**



**(b)**



**(c)**



**(d)**



**(f)**
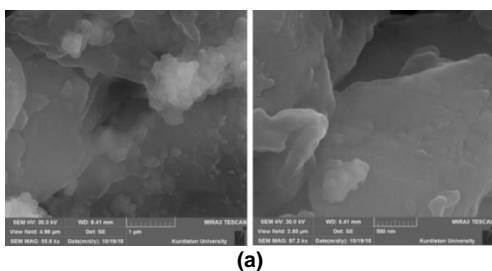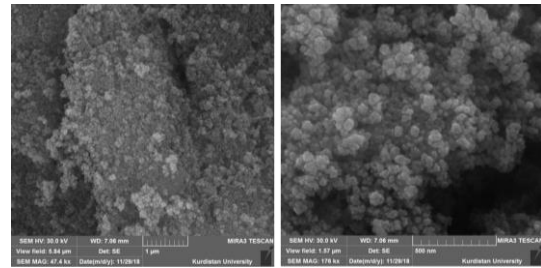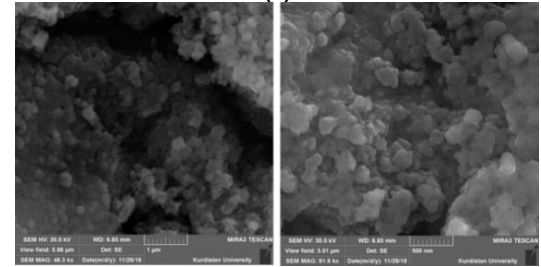
**Fig. 2.** Morphology and histogram of size of adsorbents, (a) DKP, (b) $Fe_3O_4$, (c) $Fe_3O_4$/DKP, Histogram of size of d) $Fe_3O_4$, and f) $Fe_3O_4$/DKP.

According to EDX results in Fig. 3, the Fe/C ratio in samples of A: DKP, B: $Fe_3O_4$ and C: DKP/$Fe_3O_4$ are 0, 21.40, and 4.19 and the O/C ratios are 0.23, 2.52, and 0.30, respectively. Nasser et al, 2016, conducted a chemical analysis on date palm components. they have found that the carbon content of date kernels is in the form of cellulose (32.77 %), hemicelluloses (30.20 %), and lignin (37.03 %) (Nasser et al., 2016). There are several reports about iron (Ying kong and Tanskul, 2019) or chromium (Yingkong and Tanskul, 2019, Sarkar and Sarkar, 2017) removal by cellulose. Moreover, heavy metal ions have been removed from water by lignin (Kołodyńska *et al.*, 2016). which confirm the suitability of date kernel power for iron and chromium removal. The surface morphology of DKP is very similar to that of processed Iraqi date kernels. The macropores in DKP provide a favorable space for ion interaction with the adsorbent surface, enhancing the adsorption capabilities (Nasser *et al.*, 2016).

The investigation of the surface area and porosity of $Fe_3O_4$/Date Kernels adsorbent involved the nitrogen adsorption/desorption isotherm and pore size distribution (according to BJH isotherm) curves have been attained. According to the IUOPAK classification, the adsorbent is "I" type, and hysteresis is $H_3$. Pores are slit-like cavities (slits between plates of edged particles like cubes) and non-uniform in

181

size and shape, forming a multi-domain pore size distribution, likely due to the combined nature of the adsorbent (Leofanti *et al.*, 1998). Moreover, Fig.4 shows that the average diameter of pores, in other words, the highest peak of the pores is associated with a diameter of 14.03 nm. The specific surface area of the adsorbent is 22.42 m$^2$/g, and the cumulative pore volume is 0.1659 cm$^3$/g.

The magnetic residual curve diagrams for adsorbents have been attained by a vibrating sample magnetometer (VSM). According to Fig.5, both adsorbents show paramagnetic properties. The amounts of saturated magnet in the pure $Fe_3O_4$ and $Fe_3O_4$/Date Kernels adsorbents are 67.3 emu/g and 37.95 emu/g. More than half of the magnetic property of $Fe_3O_4$ has been kept.

### 3.2. Parametric study of adsorption

The effect of pH, initial pollutant concentration, contact time, and adsorbent dosage were investigated at room temperature (298K). The operating conditions in Fig. 6 are as follows:
A) The initial concentrations for Fe (III) and Cr (VI) adsorbates are 10 mg/L and 5 mg/L, respectively, with an adsorbent dose of 2 g/l for both targets. The contact times are 20 min and 5 min, respectively.
B) The pH values for Fe (III) and Cr (VI) are 3 and 5 and the adsorbent doses are 2 g/L and 4 g/L. respectively. The contact time for both targets is 30 min.
C) The initial concentrations for Fe (III) and Cr (VI) are 20 mg/L and 5 mg/L, and the contact time is 30 min and 5 min, respectively. The pH values for Fe (III) and Cr (VI) are 3 and 5, respectively.
D) A) The initial concentration for Fe (III) and Cr (VI) is 10 mg/L and 5 mg/L, respectively, and the adsorbent dose is 2 g/L for both targets. The pH value for Fe (III) and Cr (VI) is 3 and 5, respectively.

The impacts of pH on the iron (III) or Chromium (VI) removal process are shown in Fig. 6a and Fig. 6e. The pH of the solution varied in a wide range of 3 to 11. In the case of Fe (III) adsorption, with the increase of pH from 3 to 7, adsorption increased at acidic pH because the H$^+$ ions in the solution attract the negative charge surface. In another study, it is notified that the highest iron (III) adsorption can occur in the pH range of 2.5 to 3.5. These two points are the estimated pH$_{pzc}$ of 2.5 and the initial precipitation point of iron (II) at pH ~3.5. This acidity range is where clinoptilolite is able to capture iron without precipitation or the occurrence of full surface protonation (Langman *et al.*, 2021).
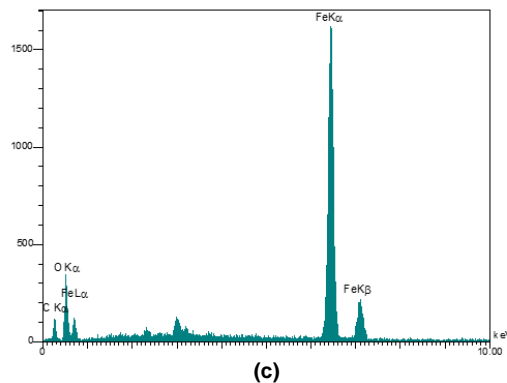
**(a)**

**(b)**

**(c)**

**Fig. 3.** EDX analysis of adsorbents *(a)* C: 81 %, O: 19%*; (b)* C: 4 %, Fe: 85.6 %, O: 10.1 %; and (c) C: 18.2 %, Fe: 76.3 %, O: 5.5 %.

As the pH increased from 7 to 9, the iron (III) precipitated as hydroxide, and sediment was observed; So, at this pH, no adsorption took place. The increase of pH to values of more than 9 caused the formed sediment to dissolve again, but the adsorption was negligible due to the rise of the hydrostatic repulsion force between iron anions and negatively charged adsorbent in large pH value.

At pH values lower than 6, the Chromium ions are namely $HCrO_4^{-1}$, $HCr_2O_7^{-2}$, $HCr_3O_{10}^{-2}$, $HCr_4O_{13}^{-2}$. Nonetheless, the dominant ion is $HCrO_4^{-1}$. At higher pH, $CrO_4^{-2}$ is the dominant ion. At low values of pH, the adsorbent was protonated and adsorbed negatively chromium anions (Alsulaili, Refaie, and Garcia, 2023; Anah and Astrini, 2017). At high pH values, the adsorbent surface was negatively charged.
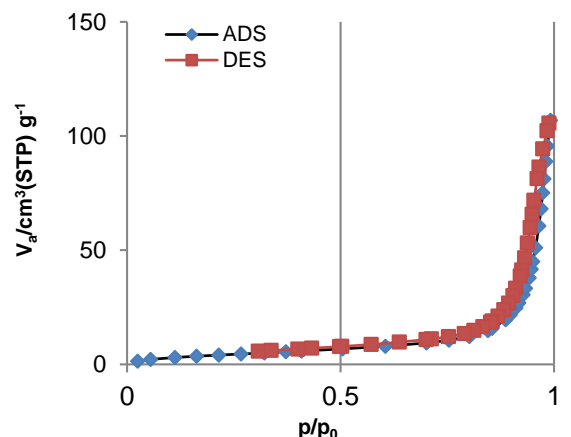
Therefore, the adsorbent repulsed the negative chromate anions. Besides, the completion between OH$^-$ and chromate ions decreases adsorption (Yingkong and Tanskul, 2019).
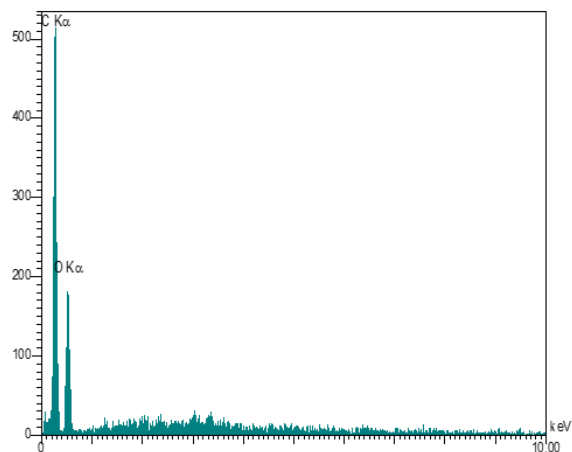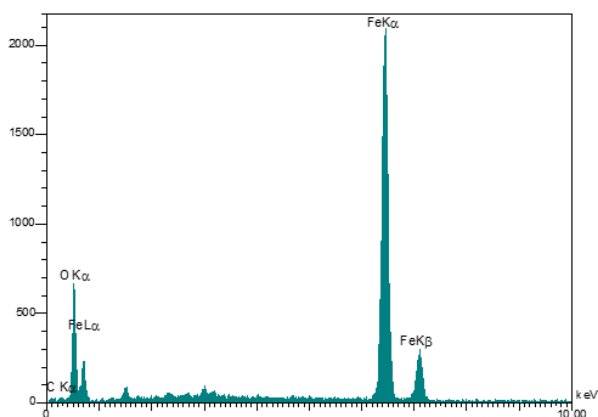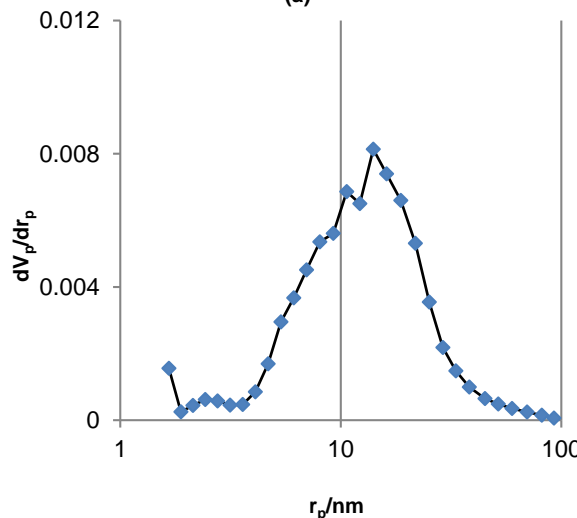
**(a)**

**(b)**

**Fig. 4.** (a) Nitrogen adsorption/desorption isotherm, (b) Pore size distribution of $Fe_3O_4$/Date Kernels adsorbent.

There is a report on date kernel as an adsorbent of thorium ions, which agrees with this work on the higher efficiencies of acidic conditions (Sarkar and Sarkar, 2017).
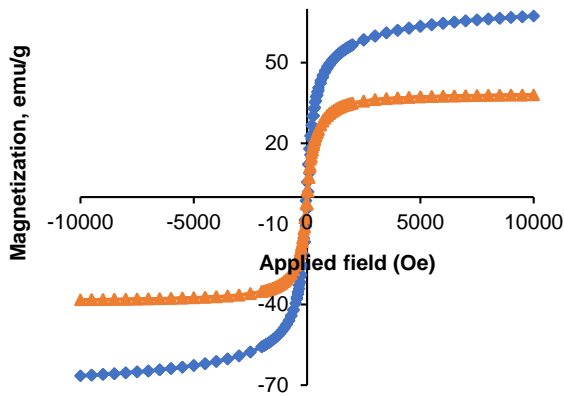


**Fig. 5.** Magnetic property of pure $Fe_3O_4$ (blue) and $Fe_3O_4$/date kernels adsorbent (Orange).

To investigate the effect of the initial concentration, tests at concentrations of 5, 10, 15, 20, and 25 mg/L, were conducted. The maximum adsorption of Fe (III) and Cr (VI) was observed at minimum concentration because of the decrease in the suitable sites for adsorption with the increase of concentration (Fig. 6b and f). The adsorbent dose has been varied from 1 to 10 g/L. From Fig. 6c, Fig. 6g, it is straightforward that for Fe (III) adsorption, with the increase of adsorbent dose to values of more than 2 g/L, Fe (III) adsorption was nearly constant. In the case of Cr (VI), for the adsorbent dose of more than 4 g/L, adsorption was almost unchanged. At an adsorbent dose of more than 2 g/L for Fe (III) and 4 g/L for Cr (VI), the solid particles aggregated because of the interaction between them, decreasing suitable surface area. Consequently, the adsorption remained constant (Chen *et al.* 2010; Heidari *et al.*, 2011).

Fig. 6d and Fig. 6h show the effects of time. The equilibrium time is 20 min for iron (III) and chromium (VI). Before equilibrium, most of the adsorption occurs via surface active sites, resulting in a high slope of the adsorption yield versus time. After equilibrium, deep active sites are saturated, and mass transfer driving force decreases leading to a slope approaching zero om the adsorption curve versus time (Kołodyńska *et al.*, 2016).

To evaluate the adsorbents for Cr (VI) removal, some experiments have been done (Fig. 7). The effect of adsorbent dosage shows that 4 g/l is the economic dosage of adsorbents. It means that after this magnitude, the increase in dosage has a negligible effect. Moreover, the performances of $Fe_3O_4$ and $Fe_3O_4$/ date kernels powder are similar and higher than DKP. A recent work reports the adsorption of $Fe_3O_4$/ date kernels powder for methylene blue adsorbent. They have a similar result, when the equilibrium dosage of adsorbent was 1 g/L (Narasimharao *et al.*, 2022). The equilibrium time is 20 min for all the adsorbents and $Fe_3O_4$ shows superior performance. In case of the effect of pH and Cr (VI), the trend of $Fe_3O_4$ and $Fe_3O_4$/ date kernel powder were similar.
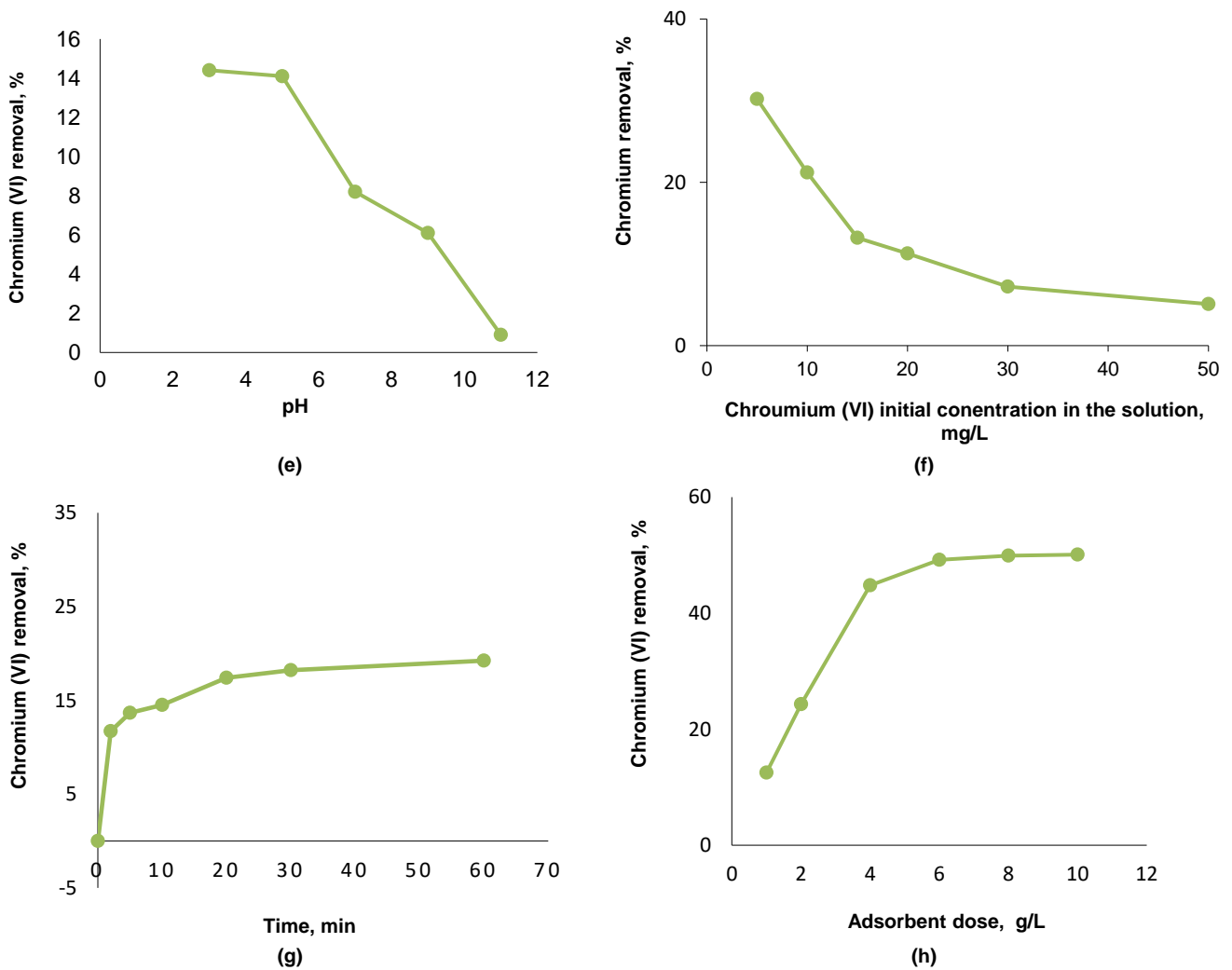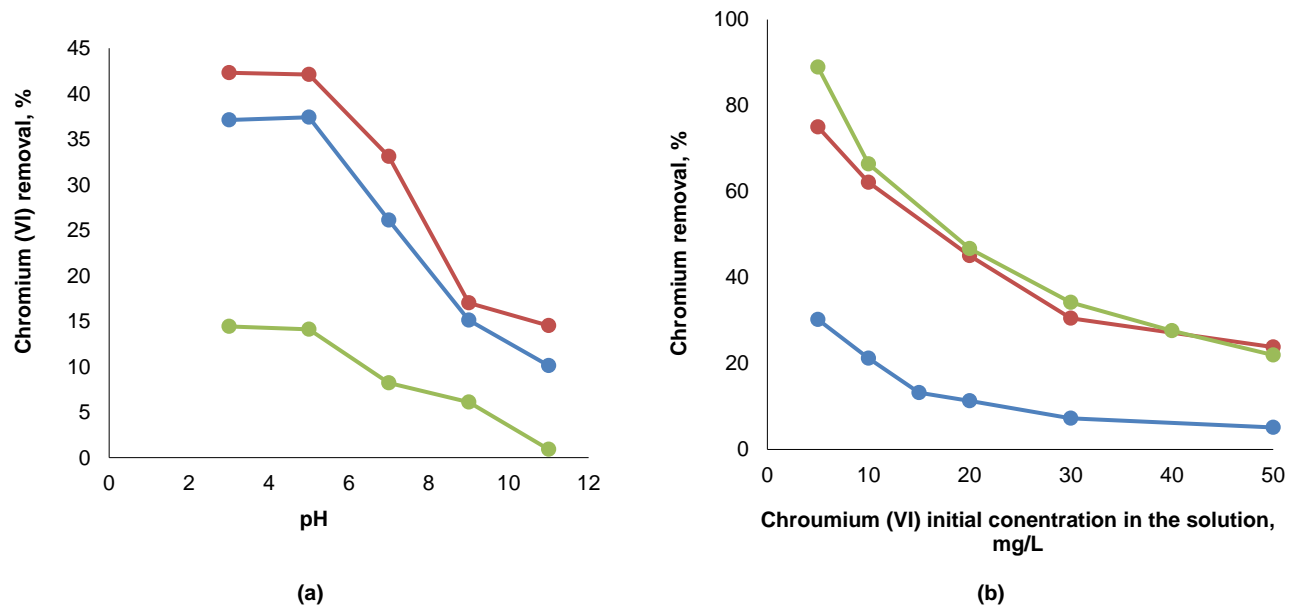


**(a)**



**(b)**



**(c)**



**(d)**
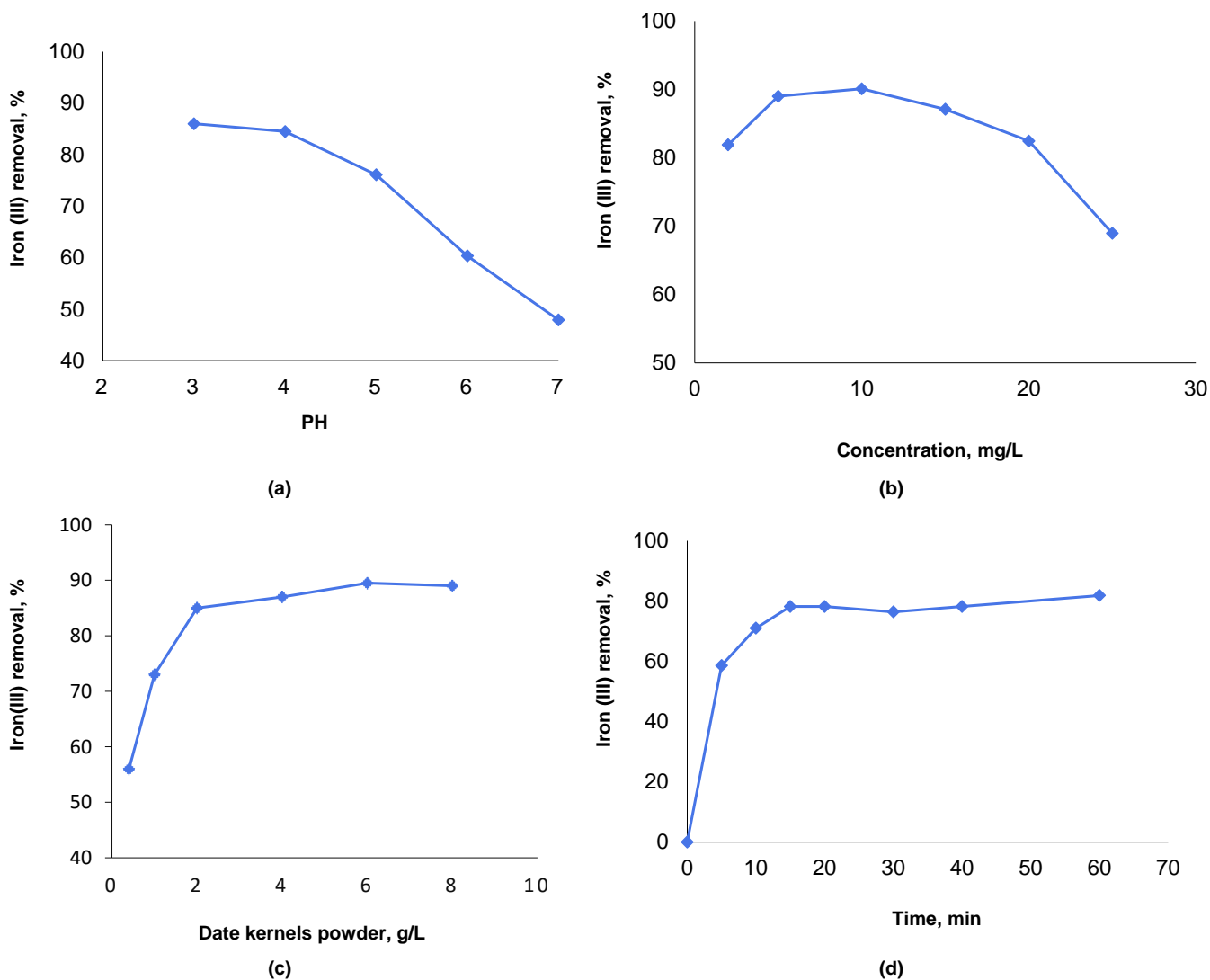
**Fig. 6.** The effects of (a) pH, (b) pollutant initial concentration, (c) adsorbent dose, (d) time of Fe (III) adsorption over DKP and the effects of (e) pH, (f) pollutant initial concentration, (g) adsorbent dose, (h) time of Cr (VI) adsorption over DKP.
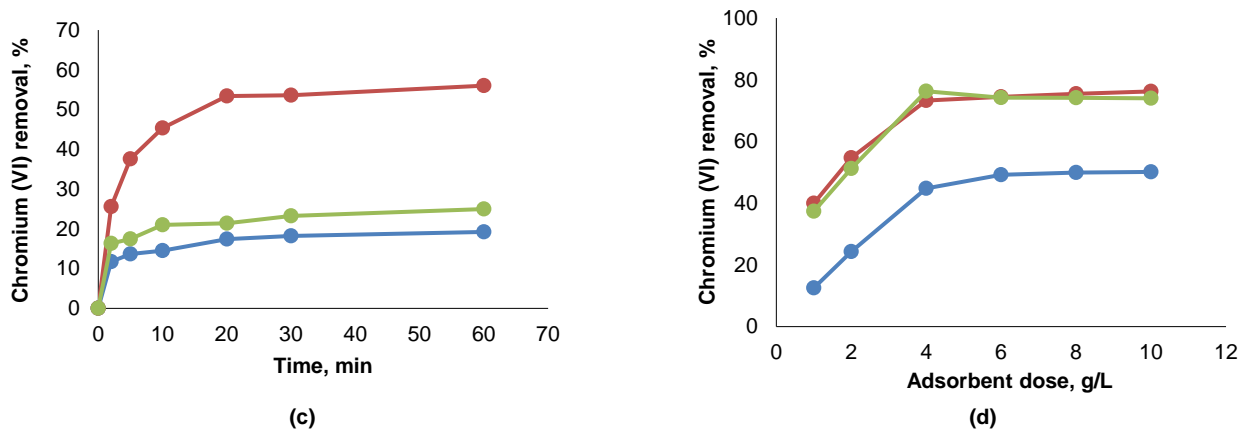
**(c)**



**(d)**

**Fig. 7.** (a) pH, (b) pollutant initial concentration, (c) adsorbent dose, (d) time of Cr (VI) removal over adsorbents (Fe$_3$O$_4$: red, date kernels powder: blue, Fe$_3$O$_4$/ date kernels powder: green).

### 3.3. Kinetics and adsorption isotherms

In this section, kinetic, thermodynamic and adsorption isotherm models were studied. The summarized results are presented in Table 2. The results of Cr (VI) and Fe (III) adsorption onto DKP, Fe$_3$O$_4$, Fe$_3$O$_4$/ Date Kernels Powder were fitted with both pseudo-first-order as shown in eq. (4) and pseudo-second-order (Eq. 5) kinetic models.

$$ln(q_e - q_t) = ln\, q_e - k_1 t \tag{4}$$

$$\frac{t}{qt} = \frac{1}{k_2 q_e^2} + \frac{1}{q_e} t \tag{5}$$

where, $k_1$ is reaction rate equilibrium constant (1/min), $q_t$ is the amount of substance absorbed per unit mass of adsorbent (g) at time t (mg∕g), and $q_e$ is the amount of substance absorbed per unit mass of adsorbent (g) at the time of equilibrium. The pseudo-second-order adsorption kinetic model had more consistency with the experimental results due to larger $R^2$ values, which enunciate that the chemical adsorption stage controlled the iron and chromium adsorption rate. The results are in agreement with (Leofanti *et al.*, 1998). Meanwhile, according to kinetics data, the adsorption of Cr (VI) ions to the surface of DKP was quicker

than Fe (III) ions. The thermodynamic modeling shows that the Gibbs free energy is negative and enthalpy change is positive, which confirms the spontaneous and endothermic nature of adsorption.

$$\frac{C_e}{q_e} = \frac{1}{q_{max}} C_e + \frac{1}{b q_{max}} \tag{6}$$

$$Ln\, q_e = Ln\, k_f + \frac{1}{n} Ln C_e \tag{7}$$

where, $q_{max}$ is the maximum adsorption capacity and b, $k_f$, and n are experimental constants. $C_e$ and $q_e$ are defined in Eq. 2.

The Langmuir and Freundlich isotherms have been given in Eqs. 6 and 7. For both Cr (VI) and Fe (III), the determining factor, $R^2$, of the Langmuir isotherm was larger than Freundlich (Table 2). The larger value and closeness to unity confirmed that the adsorption isotherm followed the Langmuir model. Langmuir isotherm for adsorption indicates monolayer and uniform adsorption of adsorbate and equally energetic sites. The maximum adsorption capacity of DKP, $q_{max}$, was 10.5 mg/g for iron (III) and 0.66 mg/g for chromium (VI), which showed higher adsorption capability for DKP toward iron (III). However, Fe$_3$O$_4$ and Fe$_3$O$_4$/Date Kernels Powder has $q_{max}$ of 10.5 mg/g and 2.88 for chromium (VI).

**Table 2.** Kinetics and adsorption isotherm models of iron and chrome adsorption.

| Model | Adsorbent | Adsorbate | Pseudo second order | | | Pseudo first order | | |
|---|---|---|---|---|---|---|---|---|
| | | | $R^2$ | $q_e$, mg/g | $k_2$, g/mg.min | $R^2$ | $q_e$, mg/g | $k_1$, 1/min |
| **Kinetics** | Date Kernels Powder | Iron (III) | 0.9986 | 4.1718 | 0.1310 | 0.6340 | 1.1146 | 0.0179 |
| | Date Kernels Powder | Chrome (VI) | 0.9988 | 0.499 | 0.785 | 0.9308 | 0.187 | 0.0425 |
| | Fe$_3$O$_4$ | Chrome (VI) | 0.9981 | 1.658 | 0.142 | 0.9191 | 0.953 | 0.0257 |
| | Fe$_3$O$_4$/ Date Kernels Powder | Chrome (VI) | 0.9986 | 1.283 | 0.335 | 0.9101 | 0.617 | 0.0169 |
| **Thermodynamic** | Adsorbent | Adsorbate | $-\Delta G\ (\frac{J}{mol.\,K})$ | | | | $\Delta H$ (J/mol.K) | $\Delta S$ $(\frac{J}{mol.\,K})$ |
| | | | **25 °C** | **35 °C** | **45 °C** | **55 °C** | | |
| | Date Kernels Powder | Iron (III) | 8225.1 | 6783.8 | 5342.6 | 3901.2 | 39050 | 144.13 |
| | Fe$_3$O$_4$/ Date Kernels Powder | Chrome (VI) | 2159.98 | 5410.75 | 8661.53 | 119112.3 | 94713.1 | 325.08 |
| **Adsorption Isotherms** | Adsorbent | Adsorbate | Freundlich | | | Langmuir | | |
| | | | $R^2$ | $k_f$ (mg$^{1-1/n}$. g$^{-1}$. L$^{1/n}$) | N | $R^2$ | $q_m$ (mg/g) | $k_L$ (L.g$^{-1}$) |
| | Date Kernels Powder | Iron (III) | 0.8456 | 3.88 | 2.02 | 0.9786 | 10.5 | 0.695 |
| | Date Kernels Powder | Chrome (VI) | 0.8456 | 0.328 | 2.02 | 0.9895 | 0.6 | 0.3 |
| | Fe$_3$O$_4$ | Chrome (VI) | 0.9632 | 1.07 | 3.1 | 0.9785 | 10.50 | 0.695 |
| | Fe$_3$O$_4$/ Date Kernels Powder | Chrome (VI) | 0.9856 | 1.287 | 4.47 | 9.9979 | 2.88 | 0.524 |

185

## 4. Conclusions

The main objective of this study was to apply date kernels powder (DKP) for the adsorption of iron (III) and chromium (VI) from water. The FTIR and EDX results showed the hydrocarbonic nature of the DKP. SEM images depicted a porous structure and rough surface of DKP. A decrease in adsorption with an increase in pH was observed for both iron (III) and Cr (VI). The kinetics of the adsorptions corresponded to the pseudo-second-order model. The adsorption isotherms followed the Langmuir model. For iron (III), the removal efficiency reached 80 %, which was obtained at the initial concentration of 10 mg / l, adsorbent dose of 2 g/L, pH of 3, and time of 30 min. In the case of chromium (VI), it was 44.8 %, which was at the operating conditions of initial concentration of 5 mg/L, pH 5, adsorbent dose of 4 g/L, pH of 5, and time of 30 min. The results showed superior iron (III) adsorption rather than chromium (VI) on date kernel powder. The findings of this work highlight the possibility of minimal use of chemicals in producing an affordable, abundant adsorbent from agricultural waste. Future research work can focus on modifying the adsorbents for better efficiency and stability tests for multiple reuses to improve their applicability on an industrial scale.

## Nomenclature

| | |
|---|---|
| WCS | World cancer society |
| DKP | Date kernel powder |
| FTIR | Fourier transform infrared |
| VSM | Vibrating sample magnetometer |

## Author Contributions

Faranak Akhlaghian: Conceptualization, supervisor, analysis of the results.
Behzad Hossieni: Performing the experiments, analysis of the results.
Somayeh Sohrabi: Writing the manuscript and editing, analysis of the results.

## Conflict of Interest

The authors declare that they have no known competing financial interests or personal relationships that could have appeared to influence the work reported in this paper.

## Acknowledgement

## Data Availability Statement

All data generated or analysed during this study are included in this article.

## References

Ahluwalia, S.S., and Goyal, D. (2007) 'Microbial and plant derived biomass for removal of heavy metals from wastewater', *Bioresource Technology*, 98(12), pp. 2243-2257. doi: https://doi.org/10.1016/j.biortech.2005.12.006

Lipps, W., Braun-Howland, E., Baxter, T. (eds.) (2005) 'American public health association, American water works association, water environment federation', *Standard Methods for the Examination of Water and Wastewater*. 21th ed. Washington DC: APHA Press.

Alsulaili, A.D., Refaie, A.A., and Garcia H.A. (2023) 'Adsorption capacity of activated carbon derived from date seeds: Characterization, optimization, kinetic and equilibrium studies', *Chemosphere*, 313, p. 137554. doi: https://doi.org/10.1016/j.chemosphere.2022.137554

Anah, L., and Astrini, N. (2017) 'Influence of pH on Cr (VI) ions removal from aqueous solutions using carboxymethyl cellulose-based hydrogel as adsorbent', IOP Conference Series: Earth and Environmental Science: 1st International Symposium on Green Technology for Value Chains 2016 3–5 October 2016, Tangerang, Indonesia, p. 012010. doi: https://doi.org/10.1088/1755-1315/60/1/012010

Bashir, M., Tyagi, S., and Annachhatre A.P. (2020) 'Adsorption of copper from aqueous solution onto agricultural Adsorbents: Kinetics and isotherm studies', *Materials Today: Proceedings*, 28, pp. 1833-1840. doi: https://doi.org/10.1016/j.matpr.2020.05.287

Bhaumik, M. *et al.* (2011) 'Enhanced removal of Cr (VI) from aqueous solution using polypyrrole/Fe$_3$O$_4$ magnetic nanocomposite', *Journal of Hazardous Materials*, 190 (1), pp. 381-390. doi: https://doi.org/10.1016/j.jhazmat.2011.03.062

Chen, S. *et al.* (2010) 'Equilibrium and kinetic adsorption study of the adsorptive removal of Cr (VI) using modified wheat residue', *Journal of Colloid and Interface Science*, 349 (1), pp. 256-264. doi: https://doi.org/10.1016/j.jcis.2010.05.057

Chernyshova, I.V., Ponnurangam, S., and Somasundaran, P. (2011) 'Adsorption of Fatty Acids on Iron (Hydr)oxides from Aqueous Solutions' *Langmuir'*, 27 (16), pp. 10007-10018. doi: https://doi.org/10.1021/la2017374

Ehralian, M. *et al.* (2016). 'Removal of Fe$^{2+}$ from aqueous solution using manganese oxide coated zeolite and iron oxide coated zeolite', *International Journal of Engineering*, 29(11), pp. 1587-159. Available at: https://www.ije.ir/article_72830.html (30 October 2023).

Fan, S. *et al.* (2020) 'Preparation of sugarcane bagasse succinate/alginate porous gel beads via a self-assembly strategy: Improving the structural stability and adsorption efficiency for heavy metal ions', *Bioresource Technology*, 306, p. 123128. doi: https://doi.org/10.1016/j.biortech.2020.123128

Ghandoor, H. E. *et al.* (2012) 'Synthesis and Some Physical Properties of Magnetite (Fe$_3$O$_4$) Nanoparticles', *International Journal of Electrochemical Science*, 7(6), pp. 5734-5745. doi: https://doi.org/10.1016/S1452-3981(23)19655-6

Gul, B., Khan, S., and Ahmad, I. (2022) '*Extraction of phytochemicals from date palm (Phoenix dactylifera L.) seeds by enzymatic hydrolysis', Journal of Food Processing and Preservation*, 46 (11), p. e17007. doi: https://doi.org/10.1111/jfpp.17007

Heidari, M. *et al.* (2011) '*Evaluation of Aluminum-Coated Pumice as a Potential Arsenic(V) Adsorbent from Water Resources', International Journal of Environmental Research*, 5 (2), pp. 447-456. doi: https://doi.org/10.22059/ijer.2011.329

Inamuddin, Ahamed, M., Lichtfouse, E., Asiri, A., (eds.) (2021) '*Agricultural Waste Absorbents for Heavy Metal Removal*, in *Green Adsorbents to Remove Metals, Dyes and Boron from Polluted Water'*, Springer International Publishing: Cham.

Jain, M. et al. (2018) 'Development of iron oxide/activated carbon nanoparticle composite for the removal of Cr (VI), Cu (II) and Cd (II) ions from aqueous solution', *Water Resources and Industry*, 20, pp. 54-74. doi: https://doi.org/10.1016/j.wri.2018.10.001

Karizaki, V.M. (2017) 'Iranian dates and ethnic date-based products', *Journal of Ethnic Foods*, 4(3), pp. 204-209. doi: https://doi.org/10.1016/j.jef.2017.08.002

Keramat, J. and Khorvash, M. (2002), 'Determination of composition of iranian dominant dates', JSTNAR, 6(1), pp. 189-198. Available at: http://jcpp.iut.ac.ir/article-1-12-en.html (1 October 2023).

Kołodyńska, D. *et al.* (2016) 'Development of New Effective Sorbents Based on Nanomagnetite', *Nanoscale Research Letters*, 11(1), p. 152. doi: https://doi.org/10.1186/s11671-016-1371-3

Langman, J.B., *et al.* (2021) 'Clinoptilolite and iron sorption/desorption under multiple pH conditions: Testing a substrate for passive treatment of acidic, iron-rich solutions', *Water Environment Research*, 93 (9), pp. 1714-1721. doi: https://doi.org/10.1002/wer.1557

Lasat, M.M (2002) 'Phytoextraction of toxic metals: a review of biological mechanisms', *Journal of Environmental Quality*, 31 (1), pp. 109-20. doi: https://doi.org/10.2134/jeq2002.1090

Leofanti, G. *et al.* (1998), 'Surface area and pore texture of catalysts', *Catalysis Today*, 41(1), pp. 207-219. doi: https://doi.org/10.1016/S0920-5861(98)00050-9

Lyons, E. (1927), 'Thioglycolic acid as a color test for iron', *Journal of the American Chemical Society*, 49 (8), pp. 1916-1920. doi: https://doi.org/10.1021/ja01407a010

Narasimharao, K., *et al.* (2022), 'Fe$_3$O$_4$@date seeds powder: a sustainable nanocomposite material for wastewater treatment', *Journal of Materials Research and Technology*, 18, pp. 3581-3597. doi: https://doi.org/10.1016/j.jmrt.2022.03.176

Nasser, R.A., *et al.* (2016) 'Chemical analysis of different parts of date palm (phoenix dactylifera l.) using ultimate, proximate and thermo-gravimetric techniques for energy production', *Energies*, 9 (5), p. 374. doi: https://doi.org/10.3390/en9050374

Omo-Okoro, P.N., Daso, A.P., and Okonkwo, J.O. (2018) 'A review of the application of agricultural wastes as precursor materials for the adsorption of per- and polyfluoroalkyl substances: A focus on current approaches and methodologies*, Environmental Technology & Innovation*, 9, pp. 100-114. doi: https://doi.org/10.1016/j.eti.2017.11.005

Pamukoglu, Y., and Kargi, F. (2006) 'Removal of copper (II) ions from aqueous medium by biosorption onto powdered waste sludge'*, Process Biochemistry*, 41 (5), pp. 1047-1054. doi: https://doi.org/10.1016/j.procbio.2005.11.010

Pavan, F.A., Mazzocato, A.C., and Gushikem, Y. (2008) 'Removal of methylene blue dye from aqueous solutions by adsorption using yellow passion fruit peel as adsorbent'*, Bioresource Technology*, 99 (8), pp. 3162-3165. doi: https://doi.org/10.1016/j.biortech.2007.05.067

Qasim, S.R., Motley, E.M., and Zhu, G. (2000) '*Water works engineering: planning, design, and operation*', 1st edition, Pearson College Div, Upper Saddle River, NJ: Prentice Hall PTR.

Saleh, M., *et al.* (2021), 'Green synthesis of zero valent iron nanoparticles using Verbascum thapsus and its Cr (VI) reduction activity'*, Bioresource Technology Reports*, 13 (1), p. 100637. doi: https://doi.org/10.1016/j.biteb.2021.100637

Salman, J.M., and Abid, F.M., (2013) 'Preparation of mesoporous activated carbon from palm-date pits: optimization study on removal of bentazon, carbofuran, and 2,4-D using response surface methodology'*, Water Science and Technology*, 68 (7), pp. 1503-11. doi: https://doi.org10.2166/wst.2013.370

Sarkar, M., and Sarkar, S. (2017) 'Adsorption of Cr (VI) on Iron (III) cellulose nanocomposite bead', *Environmental Processes*, 4 (4), pp. 851-871. doi: https://doi.org/10.1007/s40710-017-0275-2

Selvi, K., Sangma, P., and Kadirvelu, K. (2001) 'Removal of Cr (VI) from aqueous solution by adsorption onto activated carbon', Bioresource Technology, 80(1), pp. 87-89. doi: https://doi.org/10.1016/S0960-8524(01)00068-2

Shan, H., *et al.* (2021) 'Iron oxides decorated graphene oxide/chitosan composite beads for enhanced Cr (VI) removal from aqueous solution'*, International Journal of Biological Macromolecules*, 172, pp. 197-209. doi: https://doi.org/10.1016/j.ijbiomac.2021.01.060

Swank, H.W., and Mellon, M.G. (1938) 'The determination of iron with mercaptoacetic acid'*, Industrial & Engineering Chemistry Analytical Edition*,10 (1), pp. 7-9. doi: https://doi.org/10.1021/ac50117a003

Yang, Y., and Wang, P., (2006), 'Preparation and characterizations of a new PS/TiO2 hybrid membranes by sol–gel process', *Polymer*, 47 (8), pp. 2683-2688. doi: https://doi.org/10.1016/j.polymer.2006.01.019

Yingkong, P. and Tanskul, S. (2019), 'Adsorption of Iron (III) and copper (ii) by bacterial cellulose from Rhodococcus sp. MI 2'*, Journal of Polymers and the Environment*, 27 (9), pp. 1948-1958. doi: https://doi.org/10.1007/s10924-019-01480-5